Hindawi Publishing Corporation
Journal of Nanoscience
Volume 2014, Article ID 173845, 6 pages
http://dx.doi.org/10.1155/2014/173845

Research Article

Microstructural and Electrochemical Properties of rf-Sputtered $LiFeO_2$ Thin Films

P. Rosaiah and O. M. Hussain

Thin film Laboratory, Department of Physics, Sri Venkateswara University, Tirupati–517 502, India

Correspondence should be addressed to O. M. Hussain; hussainsvu@gmail.com

Received 15 August 2013; Revised 21 December 2013; Accepted 7 February 2014; Published 13 March 2014

Academic Editor: Vincent Jousseaume

Lithium iron oxide ($LiFeO_2$) thin films have been deposited by rf-magnetron sputtering technique and microstructural and electrochemical properties were studied. The films deposited at a substrate temperature 250°C with subsequent post annealing at 500°C for 4 h exhibited cubic rock-salt structure with Fm3m space group. The films exhibited well-defined oxidation and reduction peaks suggesting complete reversibility upon cycling. The as-deposited films exhibited an initial discharge capacity 15 $\mu Ah/cm^2 \cdot \mu m$, whereas the films post annealed at 500°C for 4 h in controlled oxygen environment exhibited 31 $\mu Ah/cm^2 \cdot \mu m$.

1. Introduction

The substantial development of lithium ion batteries with high energy density and capacity originates from the identification of a good cathode host that can accommodate both Li^+ ions and electrons with minimal structural changes [1, 2]. During charging, the lithium ions are deintercalated from the cathode host (e.g., $LiCoO_2$) and inserted into the van der Waals gap between the anode layers (e.g., Li). Exactly, a reverse process occurs during discharge, involving the extraction of lithium from the van der Walls gap and intercalation into the cathode at their interstitial sites. The discharge/charge balance is maintained by reduction/oxidation of reversible Co^{3+} ions to Co^{4+} and maintaining the cathode structural stability, resulting in good reversibility for longer cycles. Hence, focus has been made mainly on oxides with transition metal ions, as many of them are believed to shift valence state easily [3]. In reality, oxygen ions participate strongly in accepting the electron, a fact which can be used to tailor the voltage of a cathode. Lithium transition metal oxides $LiMO_2$ (M = Mn, Co, Ni, Fe, etc.) with the layered structure are commonly used as cathode materials for rechargeable lithium batteries [4–7]. Among various lithium transition metal oxides, $LiCoO_2$ has been most widely used as a positive electrode material [8]. But, it has many disadvantages such as high toxicity, high cost, and low practical capacity [9]. Therefore alternative compounds based on other transition metals such as Fe, which are less expensive and nontoxic than Co, have to be developed. Various types of iron-containing systems including oxides and phosphates were investigated in recent years [10]. Among them, $LiFeO_2$ has been paid more attention due to high abundance and nontoxicity of iron [11]. $LiFeO_2$ has various crystalline structures such as α-$LiFeO_2$, β-$LiFeO_2$, γ-$LiFeO_2$, layered $LiFeO_2$, corrugated $LiFeO_2$, and goethite type $LiFeO_2$ [12]. The structure of the $LiFeO_2$ mainly depends on the preparation methods. $LiFeO_2$ with various structures has been synthesized by many researchers. Galakhov et al. prepared α-$LiFeO_2$ with Fm3m space group by solid state reaction. Similarly, β-$LiFeO_2$, γ-$LiFeO_2$, layered $LiFeO_2$, corrugated $LiFeO_2$, and goethite type $LiFeO_2$ have been synthesized by various methods. Among various synthesis methods, hydrothermal synthesis is one of the simplest and best method to synthesize lithium based cathode materials [13, 14]. In the present study, α-$LiFeO_2$ was prepared using hydrothermal synthesis.

Lithium based transition metal oxides (LTMOs) in thin-film configuration with diverse structures have been the foci of the research community in the outlook of their potential applications in science and technology [15]. Deposition of stoichiometric α-$LiFeO_2$ films in single phase along with

good adhesion is a challenging problem for obtaining good reversibility. To best of our knowledge, no efforts were made to grow thin films of $LiFeO_2$. Among various physical and chemical vapor deposition techniques, rf-magnetron sputtering technique is found to be a powerful and best technique for the deposition of metal oxide thin films with reasonable stoichiometry, crystallinity, and morphology by properly controlling the essential deposition parameters [16]. The electrochemical properties of the bulk/film electrodes of different cathode materials were studied to understand the Li^+ kinetics in the host material by several authors employing nonaqueous electrolytes. But there are many disadvantages with nonaqueous electrolytes with respect to toxicity and safety concerns. The study of electrochemical performance in aqueous electrolyte has several advantages over highly toxic and flammable organic electrolytes [17]. The ionic conductivity of aqueous electrolytes is generally higher than the organic electrolytes allowing higher rates and lower voltage drops due to lower electrolyte impedance. These advantages render the use of the aqueous electrolytes in place of nonaqueous electrolytes for the primary electrochemical characterization of α-$LiFeO_2$ thin film cathodes. Hence, in the present investigation, thin films of $LiFeO_2$ are prepared by rf-magnetron sputtering technique. The microstructural and electrochemical properties of the grown films were studied.

2. Experimental

α-$LiFeO_2$ with Fm3m space group was prepared by using hydrothermal synthesis. For that, α-FOOH, $FeCl_3{\cdot}6H_2O$ (99%), and $LiOH{\cdot}H_2O$ (98%) were used as initial materials. To prepare α-$LiFeO_2$, α-FOOH was mixed with $LiOH{\cdot}H_2O$ in distilled water using a Teflon beaker to avoid reaction with the vessel. The mixture was treated hydrothermally at 25 Kgf/cm^2 for 6 h. The temperature of the autoclave was kept at 210°C. The product was washed repeatedly with distilled water to eliminate residual $LiOH{\cdot}H_2O$ and dried at 100°C for long time. The prepared powder was made as a target (51 mm in diameter and 3 mm thick) by cold pressing of the powder mixture and subsequently sintered at 800°C for 10 h. $LiFeO_2$ thin films have been deposited by rf-magnetron sputtering technique on to metalized Si and steel substrates from the prepared $LiFeO_2$ target. The system was evacuated to a base pressure of about 5×10^{-4} Pa with a turbo molecular pump backed by a rotary pump. The distance between substrate and target was about 5 cm. The rf power applied to the target was 100 W. A rotary drive mechanism was used to rotate the substrate holder to get good uniform films.

The structure of the sample was studied by Siefert X-ray diffractometer (Siefert computerized X-ray diffractometer, model: 3003 TT) with $CuK_{\alpha 1}$ radiation (λ = 1.5406 Å) source filtered by Ni thin film operated at a voltage of 40 KV and a current 30 mA at a scan speed of 0.03° s^{-1} in the 2 theta range 30–90°. The peak positions were determined precisely using RAYFLEX-Analyze software. The Raman spectra of $LiFeO_2$ in the wave number region 200 to 1000 cm^{-1} were recorded at room temperature with a Jobin Yvon (Model HR 800 UV) Raman spectrometer using an excitation wavelength of 532 (Nd:YAG laser). The laser poser on the sample was measured by a PM 100 D console with a C-series photodiode sensor (Thorlabs GmbH). The particle size and shape were observed by scanning electron microscope (SEM, HITACHI, Model: S-3400 N) operated in high vacuum mode. The composition of the sample is analyzed by EDAX (Oxford Instruments, UK). The electrochemical measurements such as cyclic voltammetry and chronopotentiometry were performed by designing aqueous electrochemical cell. The conventional type aqueous cell design consists of a three-electrode suffused cell (Pt/saturated Li_2SO_4/$LiFeO_2$). The rf-sputtered $LiFeO_2$ films coated on metalized silicon substrate are employed as working electrode (cathode). A platinum counter (anode) electrode, which acts as a reversible source and sink of lithium ions, and commercial calomel reference (Hg/Hg^+) electrode by which the electrochemical analysis was calibrated in the presence of a saturated Li_2SO_4 aqueous solution as electrolyte were employed. The CHI 608 C (CH Instruments Inc., USA) electrochemical analyzer was used for the aqueous cell measurements.

3. Results and Discussion

3.1. Microstructural Properties. Figure 1 shows the X-ray diffraction pattern of rf-sputtered α-$LiFeO_2$ thin films deposited at 250°C followed by subsequent annealing at various temperatures. It is observed that the annealing temperature significantly affects the microstructural properties of $LiFeO_2$ thin films. The as-deposited films at 250°C exhibited low intense peaks at 43.62° corresponding to (200) orientation. The films deposited at 250°C have been postannealed at different temperatures ranging from 300°C to 500°C for 4 h in the controlled oxygen environment (5 Pa). The degree of crystallization in the films gradually increased with the increase of annealing temperature. The films annealed at 500°C displayed relatively high intense predominant diffraction peak at 43.62° as shown in Figure 1, which is attributed to the Bragg reflection from the characteristic (200) lattice planes of cubic $LiFeO_2$. In addition to predominant (200) orientation, the subsequent appearance of other characteristic orientations (111), (220), (311), and (222) at 37.55°, 63.33°, 75.94°, and 79.98°, respectively, corresponding to cubic rock-salt structure with Fm3m space group. The estimated lattice parameter of the films annealed at 500°C is 4.145 Å and is in consistence with synthesized α-$LiFeO_2$ powder data (Figure 1(a)) [18].

The surface morphological analysis recorded with SEM for as-deposited and annealed films is shown in Figure 2. A flat and featureless surface morphology has been observed for the as-deposited films. An improvement in the surface morphology along with marked improvement in the grain size and shape has been observed by post annealing process in controlled oxygen environment. The annealed films exhibited roughly spherical nanograins which are in good contact with each other. The grain size of the films is observed to be increased with post annealing treatment (Figure 3) and found to be 350 nm for the films annealed at 500°C. Generally, annealing the films at higher temperatures may increase the mobility of small islands by thermally activated process

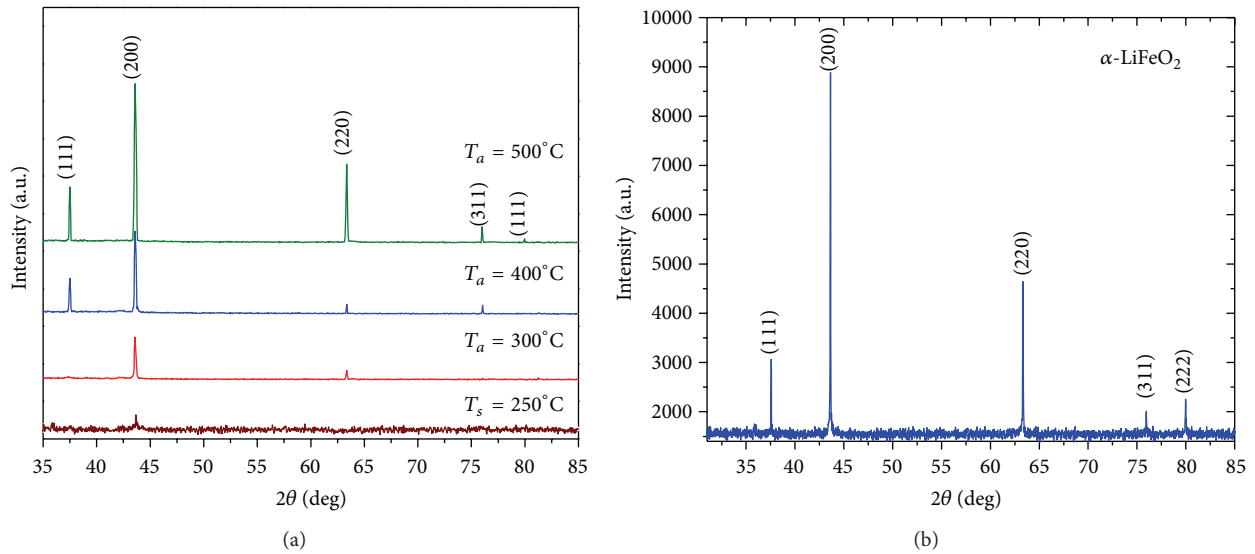

FIGURE 1: (a) X-ray diffraction spectra of as-deposited (T_s) and annealed (T_a) $LiFeO_2$ thin films. (b) X-ray diffraction spectrum of $LiFeO_2$ bulk powder.

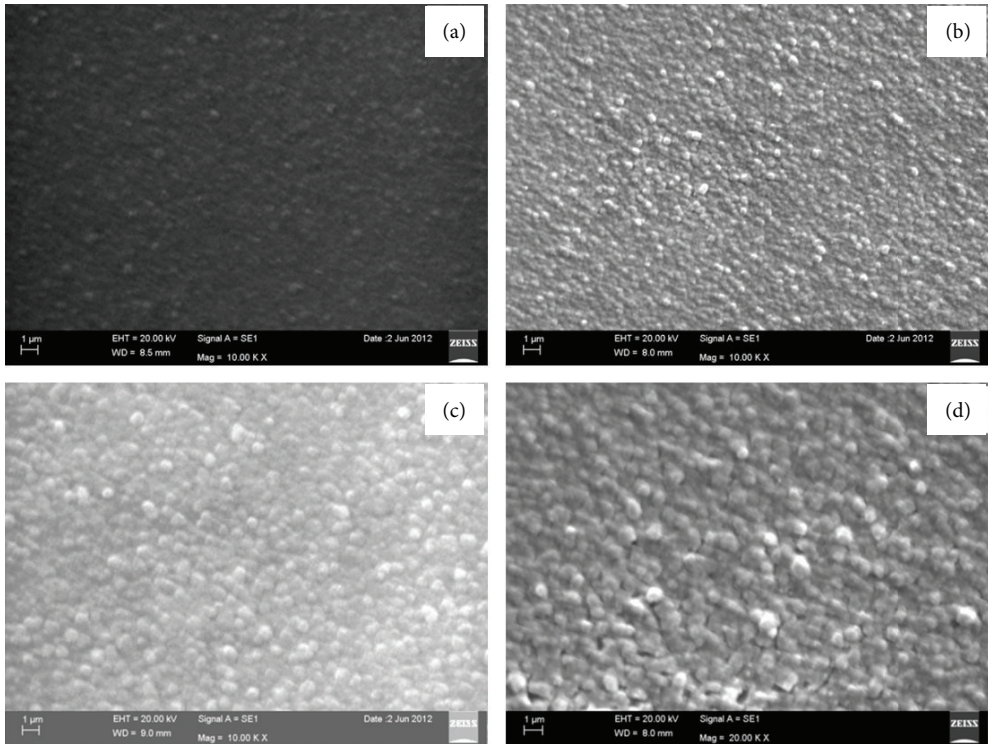

FIGURE 2: SEM images of $LiFeO_2$ films (a) as-deposited and annealed at (b) T_a = 300°C, (c) T_a = 400°C, and (d) T_a = 500°C.

and being coalesced to form a continuous film with larger grain size. Also, higher annealing temperature provides sufficient thermal energy for rearrangement of Li, Fe, and oxygen atoms to form a homogeneous film. Further increasing the annealing temperature (>500°C) may cause decomposition of the film and loss of Li or/and O.

Raman spectroscopy is an excellent analytical technique for probing the vibrational and structural properties [19]. Figure 4(a) shows the Raman spectrum of $LiFeO_2$ thin films deposited at 250°C. It exhibited two broad peaks around 540 and 650 cm^{-1}. Figure 4(b) shows the Raman spectrum of $LiFeO_2$ thin films annealed at 500°C for 4 h (T_s = 250°C). It exhibited five bands at 263, 539, 586, 655, and 709 cm^{-1}. The strongest peaks located at 539 and 655 cm^{-1} are attributed to the O–Fe–O bending and the Fe–O stretching mode of FeO_6 octahedra, respectively. The mode at low frequency,

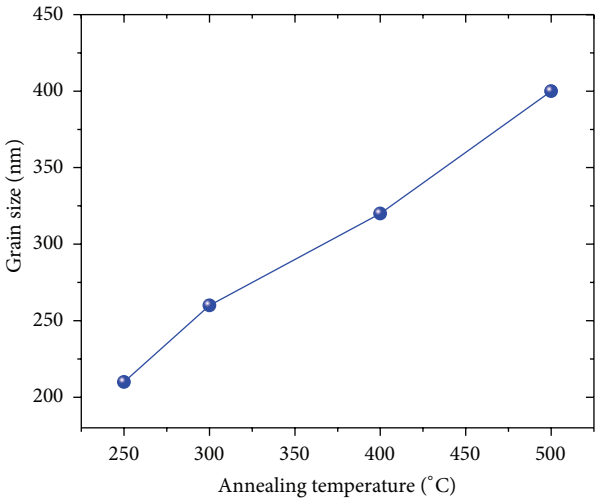

Figure 3: Variation of grain size as a function of annealing temperature.

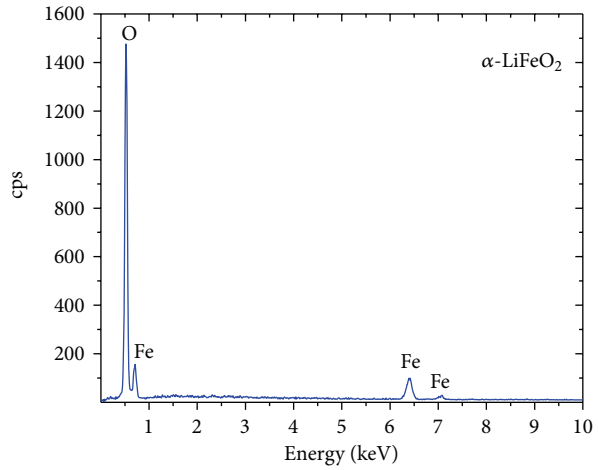

Figure 5: EDAX spectrum of $LiFeO_2$ thin films annealed at 500°C.

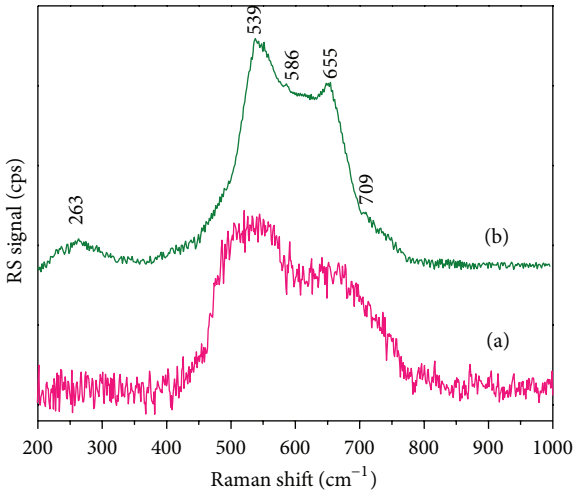

Figure 4: Raman spectra of $LiFeO_2$ thin films. (a) As-deposited, (b) annealed (T_a) at 500°C.

263 cm^{-1}, is assigned to the Li-cage in an octahedral environment and these results are in good agreement with bulk α-$LiFeO_2$ [18, 20].

The chemical analysis of the sample has been carried out using EDAX measurements and the EDAX spectrum is shown in Figure 5. The spectrum exhibited characteristic peaks of Fe and O present in the sample. It is not possible to detect Li for the obvious reason that the X-ray florescence yield is extremely low for Li. The respective peaks due to Fe and O are indicated along with their respective energy positions. The peaks due to any other elements as either impurity are not detected, which clearly indicates the sample chemical purity [18].

3.2. Electrochemical Properties. The electrochemical experiments were carried out by designing a conventional type aqueous three-electrode glass cell (Pt//$LiFeO_2$) suffused in aqueous electrolyte. Slow scan rate cyclic voltammetry was employed to study the electrochemical activity of electrodes during intercalation and deintercalation reaction. Chronopotentiometry was used to determine the specific discharge capacity and the cycling behavior of the electrodes. A $LiFeO_2$ positive electrode with an active area of 0.5 cm^2, a platinum (Pt) metal strip, and a saturated calomel electrode (SCE) were used as the working, counter, and reference electrodes, respectively. Though the Pt counter electrode may not be fully reversible in aqueous electrolyte during cycling experiment, it can have an active participation in the electrochemical process to meet higher discharge rates. The aqueous saturated Li_2SO_4 solution was used as the electrolyte. The main reason for using the saturated Li_2SO_4 aqueous solution is that the aqueous electrolyte solution processes high ionic conductivity and also reduces the electrolyte/electrode interfacial resistance [21]. The rf-sputtered α-$LiFeO_2$ thin films grown on metalized silicon substrates with subsequent post annealing from 300°C to 500°C in a controlled oxygen atmosphere were employed as positive electrodes. The electrochemical properties were systematically investigated by designing the two types of cells as mentioned in the experimental section. Slow scan cyclic voltammetry experiments were performed in saturated Li_2SO_4 aqueous electrolyte solution at a slow scan rate of 0.5 mV/s. The cyclic voltammogram exhibited a complete reversibility with perfect redox couple located at 0.29/0.38 with a peak separation of 92 mV as shown in Figure 6. The peak separation is slightly larger than the powder data. The charge/discharge capacity versus cell voltage for the Pt//$LiFeO_2$ cell derived from the constant current cycling experiments is shown in Figure 7. The aqueous cell is charged and discharged at a current density of 10 $\mu A/cm^2$ in the potential range from 0.2 V to 1.0 V. The films deposited at 250°C exhibited an initial discharge capacity of about 15 $\mu Ah/cm^2 \cdot \mu m$. This lower discharge capacity upon electrochemical cycles is due to poor crystallinity and structural instability. By annealing the deposited films at various temperatures the discharge capacity is observed to be increased, which is due to

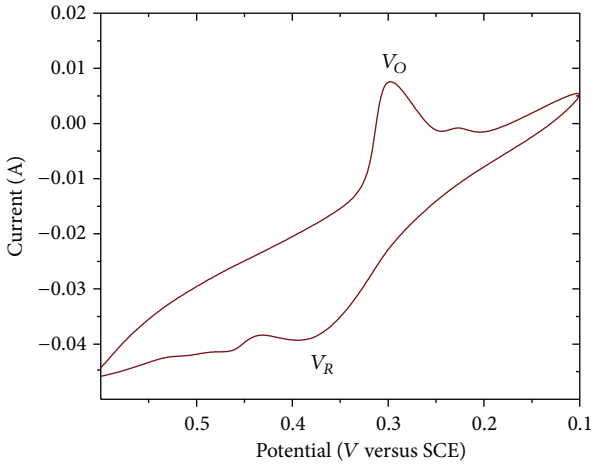

FIGURE 6: Cyclic voltammogram of Pt//$LiFeO_2$ thin films annealed at 500°C.

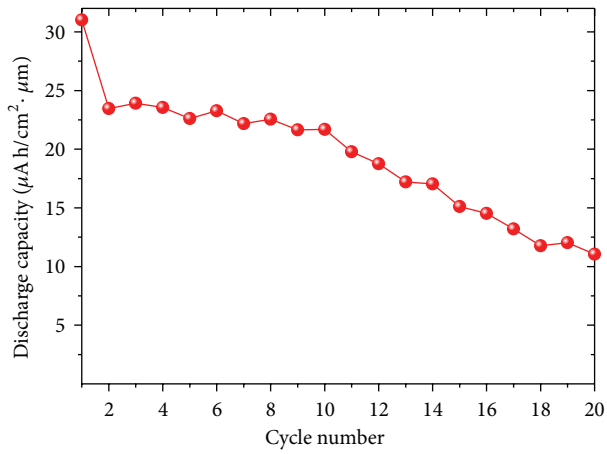

FIGURE 8: Cycling performance of Pt//$LiFeO_2$ thin films annealed at 500°C.

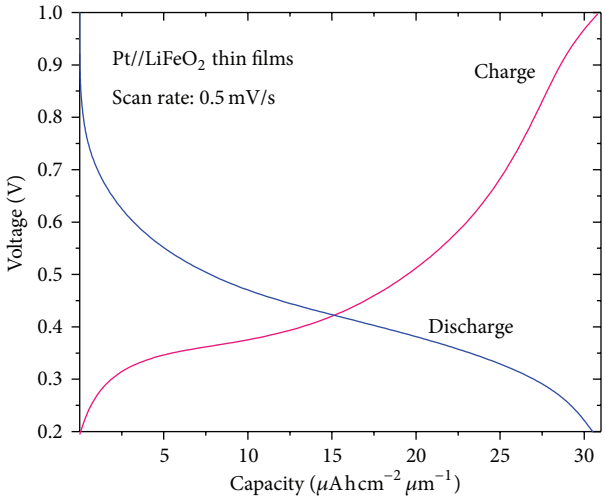

FIGURE 7: Charge-discharge curves of Pt//$LiFeO_2$ thin films annealed at 500°C.

enhancement of crystallinity [22, 23]. The films postannealed at 500°C for 4 h in controlled oxygen environment displayed a discharge capacity of 31 μAh/cm^2 · μm with good cycling behavior. It is observed that the cycling behavior for these films is stable for first 10 cycles and then gradually decreased as shown in Figure 8. The improvement of discharge capacity with annealing temperature may be due to the enhancement of grain size/surface roughness of the sample which is in consistence with microstructural analysis.

4. Conclusions

Thin films of $LiFeO_2$ deposited at 250°C by using rf-magnetron sputtering technique were annealed at various temperatures in controlled oxygen environment and their microstructure and electrochemical properties were studied. A marked improvement in the surface morphology and grain sizes was observed due to annealing. The films annealed at 500°C exhibited cubic rock-salt structure with Fm3m space group and the evaluated lattice parameter was 4.145 Å. The EDAX and Raman measurements confirm the formation of α-$LiFeO_2$ films with near stoichiometry. An improved discharge capacity of 31 μAh/cm^2 · μm with good cycling stability has been observed for the films annealed at 500°C.

Conflict of Interests

The authors declare that there is no conflict of interests regarding the publication of this paper.

Acknowledgment

The authors would like to thank University Grants Commission, New Delhi, for providing financial assistance.

References

[1] D. Li, Y. Huang, N. Sharma, Z. Chen, D. Jia, and Z. Guo, "Enhanced electrochemical properties of $LiFePO_4$ by Mo-substitution and graphitic carbon-coating via a facile and fast microwave-assisted solid-state reaction," *Physical Chemistry and Chemical Physics*, vol. 14, pp. 3634–3639, 2012.

[2] J. Su, X.-L. Wu, C.-P. Yang, J.-S. Lee, J. Kim, and Y.-G. Guo, "Self-assembled $LiFePO_4$/C nano/microspheres by using phytic acid as phosphorus source," *Journal of Physical Chemistry C*, vol. 116, no. 8, pp. 5019–5024, 2012.

[3] K.-F. Chiu, C. C. Chen, P. Y. Chen, and W.-H. Ho, "Low temperature deposition of polycrystalline lithium transition metal oxide thin films for micro batteries," *Electrochemical Society Transactions*, vol. 16, pp. 1–9, 2009.

[4] Y.-I. Jang, B. Huang, Y.-M. Chiang, and D. R. Sadoway, "Stabilization of $LiMnO_2$ in the α-$NaFeO_2$ structure type by $LiAlO_2$ addition," *Electrochemical and Solid-State Letters*, vol. 1, no. 1, pp. 13–16, 1998.

[5] S. Tintignac, R. Baddour-Hadjean, J.-P. Pereira-Ramos, and R. Salot, "High performance sputtered $LiCoO_2$ thin films obtained

at a moderate annealing treatment combined to a bias effect," *Electrochimica Acta*, vol. 60, pp. 121–129, 2012.

[6] X.-Z. Fu, X. Wang, H.-F. Peng et al., "Low temperature synthesis of $LiNiO_2$@$LiCoO_2$ as cathode materials for lithium ion batteries," *Journal of Solid State Electrochemistry*, vol. 14, no. 6, pp. 1117–1124, 2010.

[7] Y. Ma, Y. Zhu, Y. Yu et al., "Low temperature synthesis of α-$LiFeO_2$ nanoparticles and its behavior as cathode materials for Li-ion batteries," *International Journal of Electrochemical Science*, vol. 7, pp. 4657–4662, 2012.

[8] H. Xia, L. Lu, Y. S. Meng, and G. Ceder, "Phase transitions and high-voltage electrochemical behavior of $LiCoO_2$ thin films grown by pulsed laser deposition," *Journal of the Electrochemical Society*, vol. 154, no. 4, pp. A337–A342, 2007.

[9] M. Catti and M. Montero-Campillo, "First-principles modelling of lithium iron oxides as battery cathode materials," *Journal of Power Sources*, vol. 196, no. 8, pp. 3955–3961, 2011.

[10] N. Dupré, J.-F. Martin, J. Degryse, V. Fernandez, P. Soudan, and D. Guyomard, "Aging of the $LiFePO_4$ positive electrode interface in electrolyte," *Journal of Power Sources*, vol. 195, no. 21, pp. 7415–7425, 2010.

[11] T. Shirane, R. Kanno, Y. Kawamoto et al., "Structure and physical properties of lithium iron oxide, $LiFeO_2$, synthesized by ionic exchange reaction," *Solid State Ionics*, vol. 79, pp. 227–233, 1995.

[12] J. Li, J. Li, J. Luo, L. Wang, and X. He, "Recent advances in the $LiFeO_2$-based materials for Li-ion batteries," *International Journal of Electrochemical Science*, vol. 6, no. 5, pp. 1550–1561, 2011.

[13] P. Rosaiah, P. Jeevan Kumar, K. Jayanth Babu, and O. M. Hussain, "Electrical and electrochemical properties of nanocrystalline $LiFePO_4$ cathode," *Applied Physics A*, vol. 113, pp. 603–611, 2013.

[14] A. Burukhin, O. Brylev, P. Hany, and B. R. Churagulov, "Hydrothermal synthesis of $LiCoO_2$ for lithium rechargeable batteries," *Solid State Ionics*, vol. 151, no. 1–4, pp. 259–263, 2002.

[15] T. Gougousi, D. Barua, E. D. Young, and G. N. Parsons, "Metal oxide thin films deposited from metal organic precursors in supercritical CO_2 solutions," *Chemistry of Materials*, vol. 17, no. 20, pp. 5093–5100, 2005.

[16] K. Jayanth Babu, P. Jeevan Kumar, and O. M. Hussain, "Growth, microstructure and electrochemical properties of RF sputtered $LiMn_2O_4$ thin films on Au/Polyimide flexible substrates," *Materials Sciences and Applications*, vol. 4, pp. 128–133, 2013.

[17] C. Wessells, F. La Mantia, H. Deshazer, R. A. Huggins, and Y. Cui, "Synthesis and electrochemical performance of a lithium titanium phosphate anode for aqueous lithium-ion batteries," *Journal of the Electrochemical Society*, vol. 158, no. 3, pp. A352–A355, 2011.

[18] P. Rosaiah and O. M. Hussain, "Synthesis, electrical and dielectrical properties of lithium iron oxide," *Advanced Materials Letters*, vol. 4, pp. 288–295, 2013.

[19] Y. Bai, Y. Yin, J. Yang, C. Qing, and W. Zhang, "Raman study of pure, C-coated and Co-doped $LiFePO_4$: thermal effect and phase stability upon laser heating," *Journal of Raman Spectroscopy*, vol. 42, no. 4, pp. 831–838, 2011.

[20] A. E. Abdel-Ghany, A. Mauger, H. Groult, K. Zaghib, and C. M. Julien, "Structural properties and electrochemistry of α-$LiFeO_2$," *Journal of Power Sources*, vol. 197, pp. 285–291, 2012.

[21] P. Jeevan-Kumar, K. Jayanth-Babu, O. M. Hussain, and C. M. Julien, "RF-sputtered $LiCoO_2$ thick films: microstructure and electrochemical performance as cathodes in aqueous and nonaqueous microbatteries," *Ionics*, vol. 19, pp. 421–428, 2013.

[22] K. Jayanth-Babu, P. Jeevan-Kumar, O. M. Hussain, and C. M. Julien, "Influence of annealing temperature on Microstructural and electrochemical properties of rf-sputtered $LiMn_2O_4$ film cathodes," *Journal of Solid State Electrochemistry*, vol. 16, pp. 3383–3390, 2012.

[23] K. Tang, J. Sun, X. Yu, H. Li, and X. Huang, "Electrochemical performance of $LiFePO_4$ thin films with different morphology and crystallinity," *Electrochimica Acta*, vol. 54, no. 26, pp. 6565–6569, 2009.